

mHealth Technologies Toward Active Health Information Collection and Tracking in Daily Life: A Dynamic Gait Monitoring Example

Yi Cai^{id}, Xiaoye Qian^{id}, Huiyi Cao^{id}, Jianian Zheng^{id}, Wenyao Xu^{id}, and Ming-Chun Huang^{id}

Abstract—Monitoring the changes in gait patterns is important to individuals' health. Gait analysis should be taken as early as possible to prevent gait impairments and improve gait quality. Accurate stride-length estimation and gait rehabilitation activity recognition are fundamental components in gait monitoring, gait analysis, and long-term gait care. This article proposes a novel multimodality deep learning architecture to investigate the applications of stride length (SL) estimation and rehabilitation activity recognition. In order to verify this architecture, we have conducted the data collection and data labeling with our customized wearable sensing system. The sensing system can provide sensor readings from 96 sensors-based pressure array and 3-channels accelerometer and gyroscope. Many experiments with multiple perspective analysis are implemented to evaluate the models' precision, robustness, and reliability. The multimodality deep learning architecture can map multiple sensor readings to the resulting SL with a mean absolute error of 3.89 cm and accurately detect the gait activity with an accuracy of 97.08%. It correlates the step length estimation and gait activity recognition to fulfill comprehensive long-term gait information statistic. The proposed applications' implementation enriched our previous gait study and brought insights for clinically relevant wearable gait monitoring and gait analysis.

Index Terms—Active health, activity recognition, dynamic gait monitoring, footworn, multimodality, stride length (SL).

I. INTRODUCTION

A VARIETY of neurological or musculoskeletal diseases can lead to gait impairments. Particularly, poor gait and gait disorders are common in the general elderly population. It is mainly associated with the reduction of mobility [1]. Parkinson's disease patients and elder patients who have gradually lost their motor ability, experience at least one or more risk factors, including the freezing of gait, rigidity, instability of posture, balance disorders, and fall risk [2], [3]. It can be

Manuscript received 21 May 2021; revised 29 August 2021 and 19 December 2021; accepted 19 January 2022. Date of publication 28 January 2022; date of current version 8 August 2022. This work was supported by the 2021–2022 Kunshan Government Research Fund under Grant R97030024S. (Corresponding author: Ming-Chun Huang.)

Yi Cai, Xiaoye Qian, Huiyi Cao, and Jianian Zheng are with the Department of Electrical, Computer, and Systems Engineering, Case Western Reserve University, Cleveland, OH 44106 USA.

Wenyao Xu is with the Department of Computer Science & Engineering, The State University of New York at Buffalo, Buffalo, NY 14260 USA.

Ming-Chun Huang is with Data and Computational Science, Duke Kunshan University, Suzhou 215316, China (e-mail: mh596@duke.edu).

Digital Object Identifier 10.1109/JIOT.2022.3147218

more severe on affecting people's quality of life [4] and reducing their mobility if there is no effective medical interventions or gait training.

Gait analysis should be taken as early as possible to prevent gait impairments and improve gait quality. Multiple physical therapies are proposed to regain mobility, improve balance, and smooth gait. The purpose of gait training exercises is to help gait dysfunction patients to regain their mobility. The exercises are designed to improve posture, develop muscle memory, and strengthen the muscles. Gait training has great benefit to reduce the possibility of falling due to instability while walking or lowered mobility. It could allow the patients to rebuild the confidence in walking as time passes.

As many patients who suffer from gait impairments are willing to conduct a self-contained gait rehabilitation, tracking the progress of gait exercise becomes more critical, especially for the users who have minimal medical supports involved in the training procedures. Tracking the gait training performance over time can prevent overtraining and provide great support for practical training. Gait training strategies help maintain the right training intensity and volume, essential for both performance and health enhancement. Visual feedback of training data could help the medical providers and the patients evaluate the gait training performance. Training records could also drive for further gait analysis. Nevertheless, there is a great demand for a reliable mobile sensing system that could measure, document, display, and analyze relevant parameters objectively, precisely, and efficiently.

For daily exercise, stride length (SL) is an essential factor to reflect purely physical fitness and comfort [5]. SL is the distance traveled between successive points of initial contact of the same foot, i.e., the heel strike of the same foot from the starting position to the ending position. It covers two steps, one with each foot. SL could be affected by many factors, such as the height, age, illness, injuries, motion activities, and terrain of walking surface [6]. Either too-short SL or too-long SL is not appropriate to health gait training. Undesirable SL could result in awkward, uncomfortable motion states and even pull legs' muscles harmfully. SL is also a significant medical indicator to reflect gait health. Monitoring the SL while gait training exercise could help the physicians address the gait issues timely, such as gait asymmetry [7], gait stability [8]. It can also be beneficial to avoid secondary injury or risk of falling caused by rehabilitation training. SL has

TABLE I
DIFFERENCES OF THE TWO STUDIES

| Publication [11] | This study |
|---|--|
| Focus on gait analysis in terms of activities of daily living. | Focus on comprehensive gait analysis to support effective gait monitoring. |
| Proposed a series of gait parameters calculation. | Proposed Multimodality Deep learning architecture for correlated gait analysis. |
| Proposed the algorithm with stride based data segmentation. | Explored stride length estimation with under-feet pressure data and IMU data. |
| Basic daily activities. | More complex gait rehabilitation activities triggered under-feet. |
| Fundamental machine learning algorithm with features extraction for activity recognition. | Deep convolutional neural network architecture with sliding window inputs and multi-task learning framework for activity recognition and stride length estimation. |
| Dataset with six activities' data. | Stride length dataset and ten activities' dataset. |
| The experiments focus on gait parameters analysis in terms of different activities. | The experiments focus on the evaluations of proposed method for stride length estimation and rehabilitation activities recognition. |
| Data analyzing on Matlab platform, Android platform implementation | Analyzing structure with Tensorflow, results analysis via Matlab, Android application. |

also been proved the contribution of increasing gait velocity [9]. Conventional SL measurements that use a pedometer or deduction from the heights are simple and straightforward. However, they are imprecise measurements. In this study, we implement a multimodality convolutional neural network to predict the SL via, including accelerometer sensor data and under-foot ground reaction force (GRF).

Additionally, with the gait activity recognition, patients could track their gait training performance for the specific gait activity. It could also help both the physical therapists and the patients easily manipulate and record each training activity's progress. Furthermore, other important applications such that detection of unusual gait activity can provide timely alarm of the potential risks for enhanced safety and security.

Our previous studies have elaborated the characteristics of our wearable sensing system thoroughly [10] and made preliminary gait parameters and gait features investigation [11]. In this study (Table I), we extend the application for effective gait monitoring via, including SL estimation and dynamic activities classification algorithm. This research inherited the early hardware model, integrated new data sets to explore the comprehensive gait monitoring, including gait activities recognition and SL estimation with the multimodality deep convolutional neural networks. The proposed algorithm improved the application of previous wearable insole system to reflect the diversity of pedestrian walking patterns. Quantitative and qualitative gait analysis experiments with the new SL and activity data sets are implemented for supporting effective gait monitoring.

II. RELATED WORK

The research not only focuses on performing activity monitoring, it proposed a correlated gait analysis system for comprehensive long-term gait care. The combination of our proposed hardware units and algorithms for correlated step

length estimations and gait activity recognition is the main contribution of this article. Comparing to the existed gait analysis methods, the proposed system is a highly correlated gait analysis system, which include a hardware unit for high-dimensional sensor data collection and state-of-the-art algorithm support for step-length estimation and complex gait recognition.

A. Mobile Gait Analysis

With the development of mobile sensing technology, sensor-based objective mobility data analysis is increasingly developed to complete the gait exercise assessment and identify risk factors of gait rehabilitation. Conventional mobile strategies contains nonwearable and wearable. From the perspective of the hardware system, the advantages to wearable sensing systems with gait monitoring are that they are time efficient, can evaluate multiple sequential steps [12], and have the ability to evaluate the contralateral limbs within the same walking pass and in the same trial [13]. Compared to WiFi-based [14] or radar-based [15] gait monitoring, the wearable sensing systems are much easier to deploy with little environment limitations, because there should be an intensive reliable WiFi or radar networks to capture the unique variations in the channel state information to better profile human movement, which could greatly constrain human daily activity. Moreover, WiFi wireless is good for aiding position correction [16] via localization and orientation detection [17] or gait speed identification [18], but it is not enough for the nominal step length estimation or subtle gait parameters integration.

The pervasive wearable gait analysis systems are based on accelerometers (Acc) and gyroscopes (Gyro) sensor data, which have the inertial measurement units (IMUs) mounted on shoes. The IMU is usually packaged inside a small case attached on the heel of the footwear [19] or tied tightly on

the instep position of the foot [20]. Unlike traditional wearables [21], our wearable is not intrusive and comfortable since it can be flexibly worn on the body via the shoe-based design. There are important advantages of wearable sensors for the assessment of gait or balance disorders [22], which are obtaining objective measures that characterize how and why functional performance of gait and balance are impaired, increasing the sensitivity of gait measures, and increasing the opportunity for immediate biofeedback. Compared to others' works, our proposed mobile gait analysis system has advantages in integrating diversity of sensors, constructing sensor data visual feedback, and quantitative and graphical analyses. It also has a user-friendly design that all the functional sensing units are packaged inside an insole shape case, and this case can be embedded into the shoes on manufacture. Meanwhile, our proposed mobile gait analysis system has been equipped with a functional easy-use Android-based mobile software application for real-time data analysis and visualization. More details are demonstrated in the system part.

B. Combined Gait Related Stride Length Investigation and Gait Activity Recognition in Gait Analysis

In gait rehabilitation scenarios, users may experience very complex natural walking conditions. For gait impairment analysis, the transient states of gait asymmetry and gait instability are important signs to reflect its symptoms [23]. Moreover, the shuffling gait or freezing gait symptoms of Parkinson's Disease patient [24] could quickly appear and disappear, which brings a significant challenge to the physicians to focus on this issue effectively if without precise data analysis. Accurate SL estimation makes a principal contribution to solve these issues. However, conventional SL calculation methods can hardly capture the stride-by-stride variability and subtle estimation. Therefore, there are more explorations with new technologies involved, such as deep learning. Hannink *et al.* [25] claimed the first one used convolutional neural networks to estimate SL based on stride-specific inertial sensor data captured at the subject's feet. Wang *et al.* [20] proposed TapeLine, an adaptive SL estimation algorithm that automatically estimates a pedestrian's SL and walking distance using the low-cost inertial sensor embedded in a smartphone. It is constituted of the long short-term memory (LSTM) and denoising autoencoders with multimodality of Acc and Gyro readings, higher level features. They have studied the SL estimations with a variety of actions and many different smartphone-carrying methods. They have also pointed out the limitations involved in smartphone sensing for SL estimation. The difficulties are hardly ensuring that mobile phones' movement equals the movement of pedestrians and various actions result in inaccurate SL estimation.

Although most of these models or algorithms can achieve relatively higher accuracy on SL estimation, explicit confirmation of the sensor data for a specific stride interval could restrict these methods' actual application. In other words, the problem of inertial-sensor data splitting and segmentation is still an open issue in all SL estimation methods [20]. Other than the proposed studies, our system has great benefits on tracking the starting position and ending position

of the specific stride, because of the inclusion of the GRF information.

Activity recognition becomes more and more important due to its application in the fields of entertainment, industrial, healthcare, daily life, security, etc. [26]–[29]. Gait reeducation activities have been proved to improve walking endurance and gait parameters [30]. Up to date, video-based activity recognition has been explored a lot with many presented robust algorithms. However, video-based activity recognition could have many challenges, such as camera jitter, occlusions, dynamic illumination changes, and background clutter [31]. In addition to potential recognition bias, personal privacy issues can hardly be avoided while using a video camera for activity recognition. Hence, sensor-based activity recognition could have significant benefits over video-based activity recognition. Regarding sensor-based gait activity recognition, Lopez-Nava *et al.* [32] proposed recognizing gait activities via using smartphone-based acceleration data and wearable inertial sensors placed on the ankles. The proposed method that contains two stages: 1) strides detection and 2) gait classification, is accessed through five conventional activities classification. For stride detection, an acceleration signal-based algorithm is demonstrated for strides segmentation. Four conventional machine learning models are implemented to classify the specific gait activity. Compared with the work of others, our strategy has combined more gait-related sensor data, such as gyroscope data and plantar pressure data. The pitch and yaw of the gyroscope could explain the variation of body motion in a horizontal plane. The continuous changing of plantar pressure data is also significant gait information to identify particular gait activity.

III. SYSTEM

The overall system design is illustrated in Fig. 1. It contains the wearable gait lab system and the proposed multimodality deep learning structure.

A. Wearable Gait Lab System

The wearable gait lab system is built from a hierarchical structure [10]. The pressure distribution is measured via the pressure sensor array embedded inside the insole shaped package. The pressure sensor array is in an insole shape, contains 96 isolated piezoresistive sensors at most. The processing PCB board and the lithium-ion chargeable battery are packaged inside the small plastic cases separately.

All the functional units, such as the IMU, the analog-digital converter (ADC), the microcontroller, and the Wifi-Bluetooth module, are mounted on the processing PCB board. The pressure sensor is designed based on the piezoresistive principle. Each pressure sensor on the sensor array is scanned, and its value is sent to the voltage divider via multiplexer control. The IMU can collect Acc and Gyro data with a predefined sampling rate. The microcontroller plays the role of enabling or disabling every functional unit. The lithium battery takes the responsibility to provide a stable 5-V power supply for all the components.

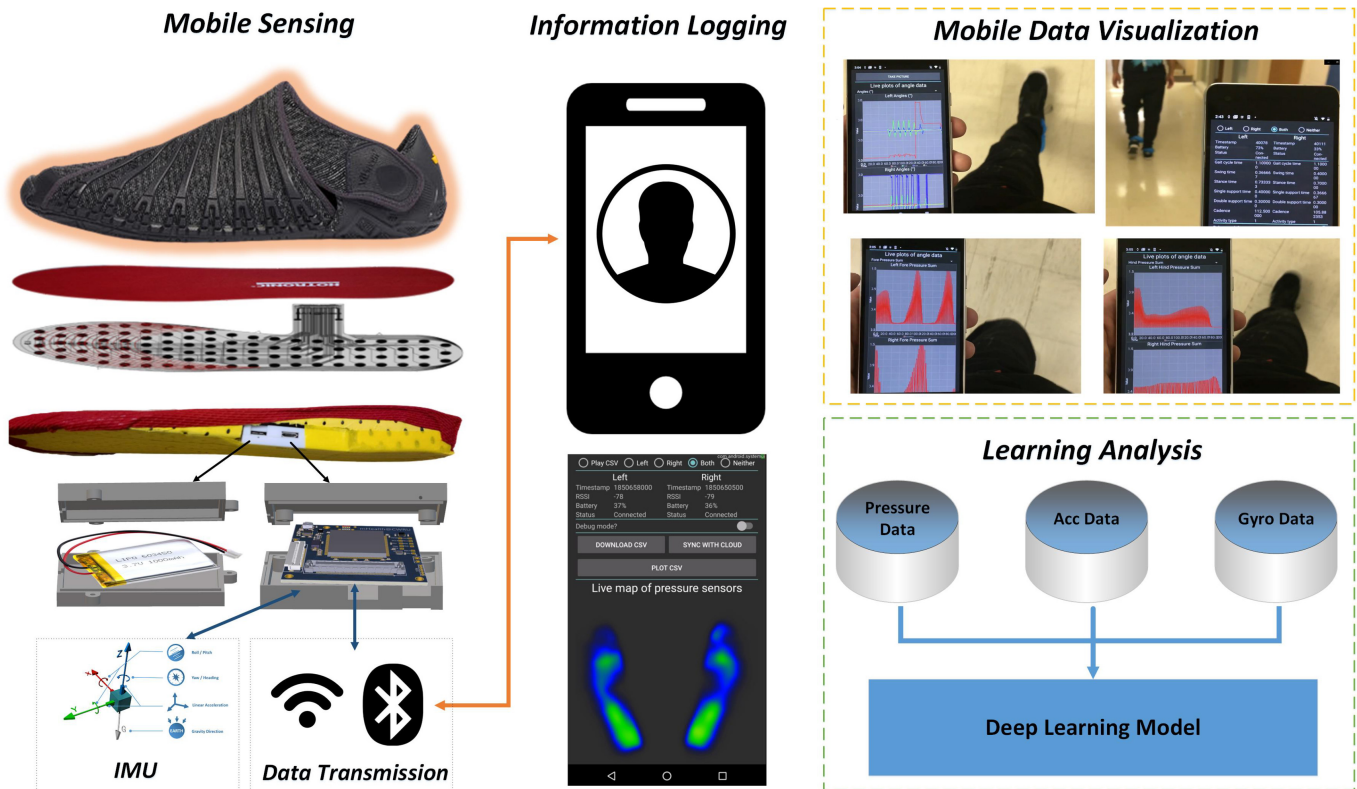


Fig. 1. Architecture of the overall system design. It is constructed by four functional units (mobile sensing, information logging, mobile data visualization, and learning analysis).

This design could significantly avoid the looseness of that the sensors are mounted outside the footwear. By hiding all the sensors inside, users would be willing to wear it due to its neat outlook and few irritations. Moreover, the pressure sensing and IMU sensing are assembled separately in the insole-shape structure, which provides constant high spatial sensing resolution. The user-friendly design manifested in that all the pressure sensors are customizable, making it feasible to trim to fit most footwear sizes from 5.5 U.S. to 14 U.S.

The sensor data are then transmitted wirelessly via Bluetooth or Wifi at a sampling rate of 30 Hz. On the receiver end (i.e., the mobile devices), an Android App is provided. This App offers a primary user interface (UI). The information of hardware connections, power consumption, timestamp tracking, and real-time plantar pressure distribution could be displayed on the main UI. In light of IMU data visualization and ordinary gait features analysis, a drag down UI is implemented [11]. It manifests the logs of gait cycle time, swing time, stance time, and plots of the sum of pressure values, IMU data, etc.

B. Exploration of Stride Length Estimation and Activity Classification

Two new applications are investigated in this study: 1) stride-length estimation and 2) rehabilitation activity classification.

SL refers to the distance traveled during the walking motion of the same foot. As shown in Fig. 2, it is the distance from the

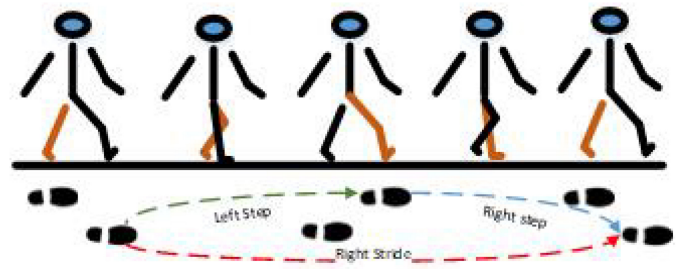


Fig. 2. SL is defined by the distance between consecutive heel strikes of the same foot, while the step length is defined by the distance between positions of opposite feet. The heel pressure is calculated by the sensor values in the hind part of the entire foot [11].

heel strike of the right foot (starting position) to the heel strike of the right foot (ending position). A step length is a distance covered by one step. It begins with the heel strike of one foot to the heel strike of the other foot. In this study, we focus on the stride segmentation of the heel-strike event. We find each stride's borders via the consecutive heel strikes that are reflected by the changing of under-feet pressure (Fig. 3). To ensure the equally scaled and fixed size input to the network, we zero-padded the sensor samples of the stride at its head and tail equally. For each sample, if it has a scale of value less or greater than the size of 45, it is interpolated to a fixed size of 45.

In terms of rehabilitation activity recognition, there are ten activities covered in this study, as shown in Fig. 4. They are

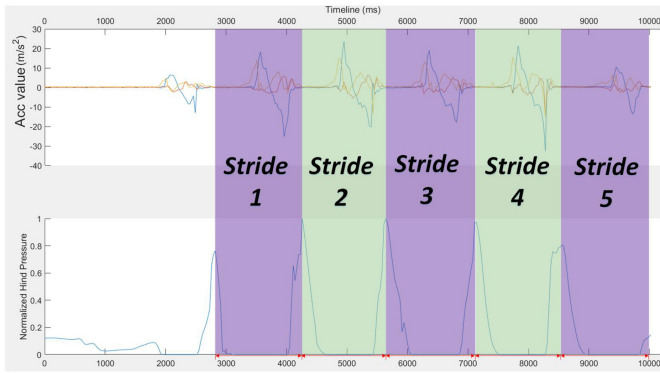


Fig. 3. Graph of acceleration and heel pressure over time. The blue, red, yellow lines indicate the accelerations in the directions of x, y, and z separately. The heel pressure is obtained from the average value of the sensor data of the heel.

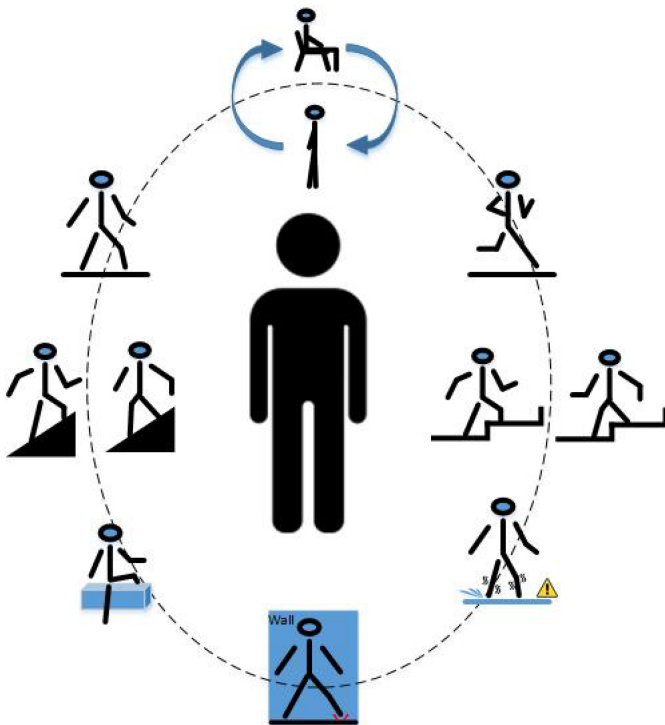


Fig. 4. Ten dynamic activities: sit-to-stand, normal walking, jogging, go upstairs or downstairs, go up-ramp or down-ramp, side-step walking, overcoming obstacles, and walking on a slippery floor.

all dynamic activities: sit-to-stand, regular walking, jogging, side-stepping, upstairs, downstairs, upward trail, downward trail, stepping over an obstacle, and walking on a slippery floor. For different activities, there are typical traits, such as the postures difference in Fig. 5. The postures difference can cause significant differences in the value of “foot contact pitch” [33] or under-feet pressure distribution, which can be reflected through the wearable sensor data. For instance, there is an obvious difference of motions on foot for activities of “walking,” “upstairs,” and “downstairs.” Typically, the forefoot position is lower than the hind foot while descending stairs but opposite while walking. While ascending stairs, the forefoot presents a flat strike when contacting the floor, and the hind



Fig. 5. Characteristics for some dynamic gait activities. The pitch angles’ changing for activities of regular walking, jogging, upstairs, downstairs, and stepping over obstacles. Motion characteristics of side-step walking and walking on a slippery floor.

foot has greater pitch angles. For jogging, instead of the double support phase, there is a dual float phase that both feet are in the air [34], and the pitch angle of heel strike might be greater than walking. When walking on a slippery ground surface, people may worry about balance. They usually step short distances and step cautiously via placing the entire foot on the ground, such as a flat foot strike instead of heel striking [35], [36]. It helps to control the balance better and avoid slipping. For the activity of “stepping over obstacles,” people often lift their legs high enough and far enough to clear the front and back edges of the obstacle [30]. The complete set of movements includes twisting the supporting leg to leave more space and raising the heel to complete the crossing. The routine activity of “side-stepping” usually requires that subject is standing tall, heading up, looking straight, and keeping their toes pointing forward [37]. Hence, the proposed characteristics could be used to discriminate the activities. The data sampling of activity recognition is based on the sliding window method. We use a 2-s window that contains 50% sample to sample overlap to determine the sample.

C. Multimodality Deep Learning Approaches Implementation

For the learning analysis, we describe a novel approach to estimate the SL and classify the activity using multimodality deep convolutional neural networks. The model for SL estimation is a regression model that maps both the Acc data and under-foot pressure sensor data of specific stride to the resulting SL. The model for activity recognition is a classification model that maps the sequence of Acc data, Gyro data, and under-foot pressure sensor data to an activity type.

The raw sensor data collected from the sensing system was preprocessed with transformation, filtering, and zero-padding before fed into the deep learning model. Due to the raw sensor readings from accelerometers inevitably contain noise and gravity value, we use a band-pass filter to transfer it into physical unit data via eliminating the acceleration noise of all three dimensions.

Our proposed models are implemented using Pytorch [38]. Table II summarizes the hyperparameters of the models. Fig. 6 displayed the architectures of multimodality deep convolutional neural networks. The regression model on the left is used for SL estimation, and the classification model on the right is used for rehabilitation activity recognition. The model

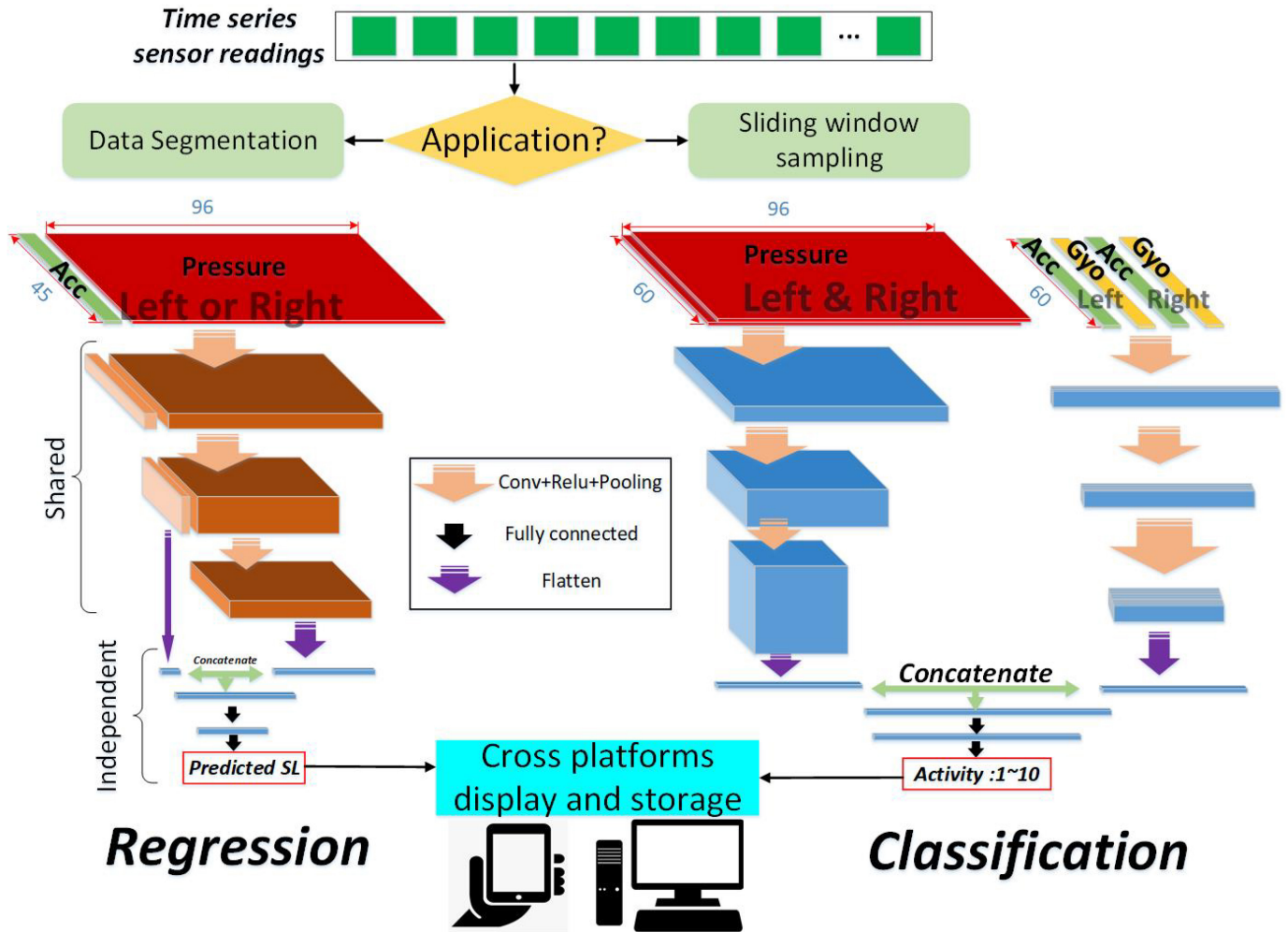


Fig. 6. Architectures of the multimodality deep convolutional neural networks. The left one is the regression model for SL estimation; the right one is the classification models for activity recognition.

TABLE II
LIST OF MODELS' HYPERPARAMETERS

| Hyper-parameters | Regression Model | Classification Model |
|-------------------------------|----------------------------------|-----------------------------------|
| Feature maps in hidden layers | (1,3)-(8,32) -(16,64)-(32,xx) | (2,12)-(6,18) -(12,36)-(24,72) |
| Activation function | Relu | LeakyRelu |
| Learning rate | 0.001 | 0.001 |
| Optimizer | Adam | Adam |
| Loss function | MSE | CrossEntropy |
| Batch size | 1 | 10 |
| Epochs | 150 | 100 |

takes parallel inputs from IMUs and pressure sensor readings. The 1-D convolutional kernels are applied to Acc and Gyo channels. The 2-D convolutional kernels are applied to pressure channels, because we not only want the model to learn signal features from the perspective of timeline but also want it to learn the pressure sensor array's spatial features. The convolutional layers are used to extract the features, project

the source data to the hidden feature domains, and condense the feature maps. The fully connected layers are much like a classifier. It projects the features from the hidden feature domains to the target domain.

The regression model is trained with inputs of sensor readings from either the left side or right side. Considering the task of estimating left SL and estimating right SL are much similar, we could use the same feature extraction architecture to process the symmetric sensor readings. Hence, the knowledge of transfer learning and multitask learning is used in this study. We construct the same convolutional layers to extract the feature maps from left and right sensor readings. The fully connected layers at the output are implemented and updated separately, which means that there are shared and independent parts for left sensor readings and right sensor readings. Through this design, we have achieved knowledge transfer between similar tasks. It is much helpful to get a robust model with limited training data.

Comparing to the regression model, the classification model has much similar structure at the shallow hidden layers, but different implementation at the decoders. On the other hand, classification model takes three kinds of sensors data from

double feet as the inputs. Same sensor readings from left and right sides as separate feature channels are stacked together to form the model inputs. Specifically, the preprocessed inertial sensor data $d_{i,j}$ and pressure sensor data $p_{i,j}$ with $i = 1, \dots, M$ channels and $j = 1, \dots, N$ samples are the inputs of the network. $d_{i,j}$ contains Acc and Gyro data from left and right as shown in (2), and $p_{i,j}$ contains pressure data from left and right

$$d_{i,j} = \begin{bmatrix} gx_j^l, gy_j^l, gz_j^l, ax_j^l, ay_j^l, az_j^l \\ gx_j^r, gy_j^r, gz_j^r, ax_j^r, ay_j^r, az_j^r \end{bmatrix} \quad (1)$$

$$p_{i,j} = \begin{bmatrix} p_j^l, p_j^r \end{bmatrix} \quad (2)$$

where l indicates left sensor readings and r indicates right sensor readings. The convolutional layers have $\lambda = 1, \dots, K$ kernels. $\kappa_{\lambda,i,j}^{(1)}$ indicates the 1-D convolutional kernels, and $\kappa_{\lambda,i,j}^{(2)}$ indicates the 2-D convolutional kernels. Activate function ν is applied to the feature maps with bias terms $b_{\lambda}^{(1)}$ and $b_{\lambda}^{(2)}$ separately to generate the output

$$\begin{aligned} z_{\lambda}^{(1)} &= \nu \left(\left(\sum_j^N \kappa_{\lambda,i,j}^{(1)} \times d_{i,j} \right) + b_{\lambda}^{(1)} \right) \\ z_{\lambda}^{(2)} &= \nu \left(\left(\sum_j^N \kappa_{\lambda,i,j}^{(2)} \times p_{i,j} \right) + b_{\lambda}^{(2)} \right). \end{aligned} \quad (3)$$

Then, the concatenated outputs feed into the fully connected layers to reach the estimate of the target variable. Fig. 6 and Algorithm 1 summarize the detailed implementation of this architecture.

The evaluation metrics for the regression model are the mean square error (MSE) and mean absolute error (MAE)

$$E_{\text{MSE}} = \frac{1}{n} \sum_{i=1}^n (\text{SL}_r^i - \text{SL}_e^i)^2 \quad (4)$$

$$E_{\text{MAE}} = \frac{1}{n} \sum_{i=1}^n (|\text{SL}_r^i - \text{SL}_e^i|) \quad (5)$$

where SL_r^i and SL_e^i denote the actual SL of the i th stride and the predicted SL, respectively. n denotes the total number of samples in the test set. MAE is a more direct representation of the sum of error terms, because it treats all errors the same in sum, however, MSE gives larger penalization to prediction error.

Conventionally, accuracy, confusion matrix, and precision and recall values are used to evaluate the classification model.

IV. EXPERIMENTS AND EVALUATIONS

A. Data Collection and Labeling

Ten participants (including seven males and three females) enrolled for data collection for SL estimation. Each subject is asked to walk ten steps for a single experiment and repeat it ten times. The subject is asked to walk on the white background, so that we use a long white paper roll for each experiment. A highlighter is tied at the lateral side of the shoes while the subject is walking. Once the subject's foot contacts the ground, the highlighter will mark a point on the white paper roll as

Algorithm 1 Implementation of Multimodality Deep Learning Architecture

Input: Time series sensor readings from left and right wearable sensing shoes.

Output: Type of rehabilitation activity (1-10) or side based stride length estimation (y^l, y^r).

/* Initialization*/

Regression model: Create network left, network right, and shared network.

Classification model: Create network with multimodality layer, hidden convolutional layers, and output fully connect layers.

/* Model train*/

if Stride length estimation **then**

for Each Stride **do**

Step 1: Extract Acc and Pressure sensor readings. Extract the corresponding ground truth as label. (Left and right train data with actual stride length $((x_i^l, x_i^r, t_i^l, t_i^r), i = 1, 2, \dots, k)$, test data without actual stride length.)

Step 2: Padding zeros equally at the head and tail of the sample.

Step 3: Extract left or right information.

if Left **then**

Step 4: Put input (x_i^l, t_i^l) into network left.

else

Step 4: Put input (x_i^r, t_i^r) into network right.

end if

Step 5: Put output m_i from Step 4 into shared network.

Step 6: Get predicted value y_i .

Step 7: Calculate $\text{MESLoss}(y_i, t_i)$ and optimize the model via backpropagation.

if Left **then**

Step 8: Weights of network left and shared network get updated.

else

Step 8: Weights of network right and shared network get updated.

end if

end for

else

for Each sliding window sample **do**

Step 1: Extract Acc, Gyo (agi) and Pressure (pi) sensor readings. Extract the corresponding ground truth as label (t_i). ($i = 1, 2, \dots, k$)

Step 2: Stack left and right inputs.

Step 3: pi go through 2D convolutional network, agi go through 1D convolutional network.

Step 4: Get predicted value y_i .

Step 5: Calculate $\text{CrossEntropyLoss}(y_i, t_i)$ and optimize the model via backpropagation.

end for

end if

/* Model test*/

Regression model: Step 1 to 6.

Classification model: Step 1 to 4.

the ground truth (GT), shown in Fig. 7. Then, the SL data are manually labeled via tape measurement straightforwardly. During each experiment, the participant started from standing still, gone through the acceleration of walking, stable walking, deceleration of walking, and back to standing still eventually. Hence, comparing to existing works [39], our SL data set covers various SL, scenarios of stride variation, and SL from both left and right foot. Besides, the addition of pressure sensors introduces more feature information. The data diversity could make the model more robust.



Fig. 7. Experiment setup of data labeling via the color pen at the side of each shoe. The SL ground truths are manually measured via tape measurement.

TABLE III
NUMBERS OF STRIDES ARE COLLECTED FROM EACH SUBJECT

| Subject ID | Number of strides |
|------------|-------------------|
| 1 | 110 |
| 2 | 119 |
| 3 | 90 |
| 4 | 98 |
| 5 | 101 |
| 6 | 100 |
| 7 | 119 |
| 8 | 96 |
| 9 | 100 |
| 10 | 97 |

TABLE IV
STATISTICAL MEASUREMENTS OF THE SL DATA SET

| Statistical Features | Values |
|----------------------|--------|
| Mean | 116.81 |
| Standard Deviation | 29.33 |
| Maximum | 169.10 |
| Minimum | 27.50 |

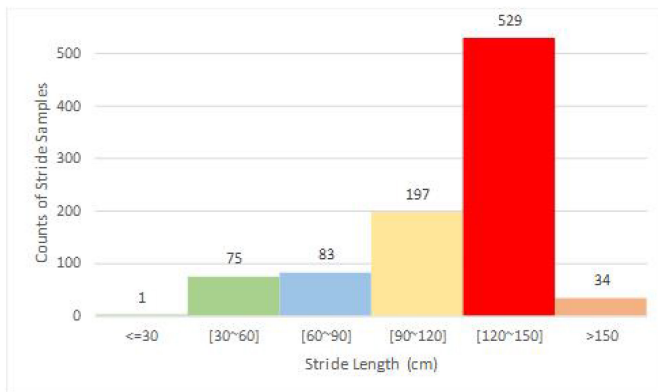


Fig. 8. Distribution of the SL samples.

After the stride segmentation, 1013 stride samples are collected totally. Table III summarizes the numbers of strides are collected from each subject and Table IV summarizes the statistical measurements of the SL data set. Fig. 8 presents the distribution of the SL samples.

For gait reeducation activity recognition, data collection from ten healthy subjects (aged between 23 and 32, height

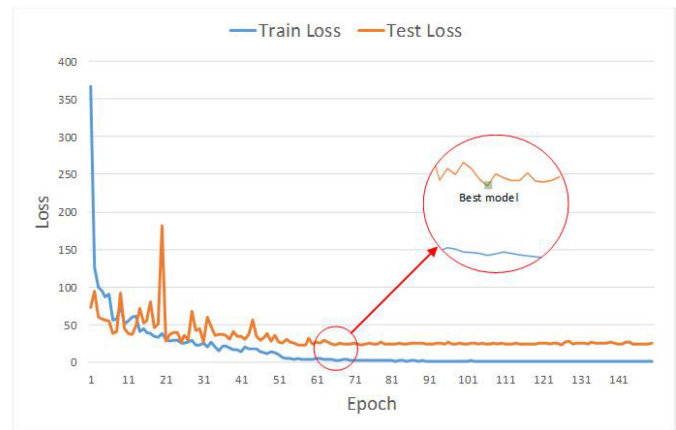


Fig. 9. Variations of SL estimation loss with respect to train and test data sets.

between 172 and 188 cm, and weight between 65 and 90 kg) with natural activity patterns that have been proposed in the system part. All of these exercises are performed on the safe walkway.

The side-stepping begins by standing sideways at one end of the walkway with the feet shoulder-width apart, in a quiet neutral position. Subjects were asked to take a few steps along the wall at a normal comfortable pace. When performing stepping over obstacles, a 60-cm height box is placed in the hallway as the obstacle. The subject is asked to cross it back and forth ten times for one set of data collection.

Collected sensor data (under-foot pressure sensors, Acc, and Gyro) have been preprocessed by sampling in fixed-width sliding windows of 2 s and 50% overlap ratio. (there are 60 readings per window). For the period that is not part of the phase of interested activity, all those ranges of values are discarded. For instance, during the walking phase, subjects have to stop and turn back at the end of the hallway. The turns are redundant activities that should not be included in the phase of walking.

B. Stride Length Estimation

To avoid the model is overfitting to the left or the right train, the train set comprises a randomly selected equal number of left foot samples and right foot samples. The remaining data constitutes a test set. The test set is composed of 53 left stride samples and 50 right stride samples.

Fig. 9 displays variations of SL estimation loss concerning train and test data sets. As shown in the figure, the model fits the train set gradually iteration by iteration. However, the testing loss decreases to the minimum value after certain iterations and then slightly increases back again. At the highlighted point in green, the model has the smallest loss to the test set. Once surpass that point, although the model can fit even better for the train set, the performance on the test set is getting worse. This situation can be explained by the overfitting issue. Hence, we take the model at the highlighted point as our final model. Fig. 10 presents the actual measurements and the estimated values of the test set directly. To analyze the agreement between the two groups, we use the Bland–Altman plot as

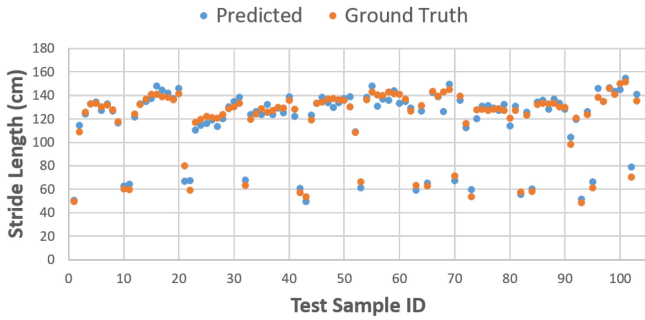


Fig. 10. Results between measured (GT) and estimated (predicted) SL via pointwise comparison.

TABLE V
MSE EVALUATION OF LEAVE-ONE-OUT TESTING

| Test ID | MSE (cm^2) |
|----------|----------------|
| 1 | 26.075 |
| 2 | 31.894 |
| 3 | 24.972 |
| 4 | 34.554 |
| 5 | 29.365 |
| Averaged | 29.372 |

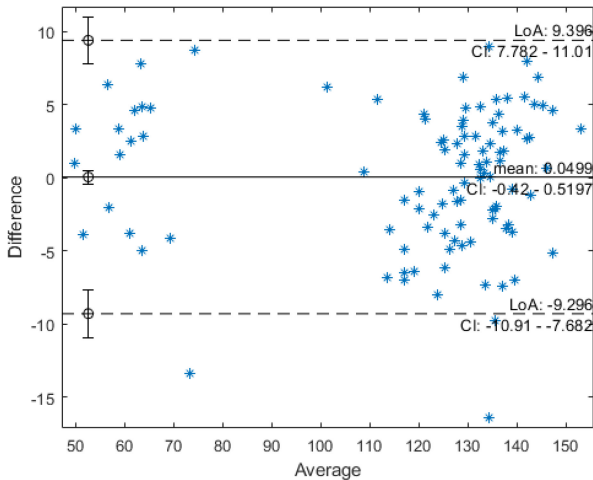


Fig. 11. Bland–Altman plot from the evaluation of results. “LoA” indicates the limit of agreement. It is usually defined by three times of the standard deviation. Each “CI” is its corresponding confidence interval of the LoA.

shown in Fig. 11. In this figure, the y-axis is the measurement error that is computed via equation $y - y_{GT}$ and the x-axis is measurement agreement that is calculated via equation $(1/2)(y + y_{GT})$. From this figure, we can find that there are only three outliers, the mean value is close to 0, and most of the samples are between the lower and upper limits of agreement. It indicates that the predicted values have a very good agreement with the actual measurements.

To investigate the model’s robustness from subject to subject, we randomly select one subject’s data as a test set, and the rest subjects’ data are used for training. We run the method five times. As shown in Table V, five experiments are implemented, and the MSE is summarized as evaluation.

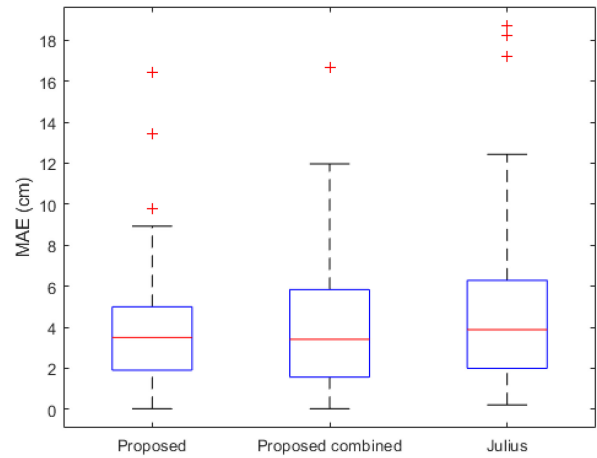


Fig. 12. Box plots of SL estimation errors. In the plot, the central red mark is the median, and the edges of the box are the 25th and 75th percentiles. Red cross marks are some outliers.

TABLE VI
RESULTS OF LISTED APPROACHES FOR SL ESTIMATION

| Method | Input Sensor Data Types | MAE (cm) | MSE (cm^2) |
|-------------------|-------------------------|--------------|----------------|
| Proposed | Pressure, Acc | 3.89 | 22.52 |
| Proposed Combined | Pressure, Acc | 4.1 | 27.26 |
| Julius [40] | Acc | 4.6 | 35.4 |

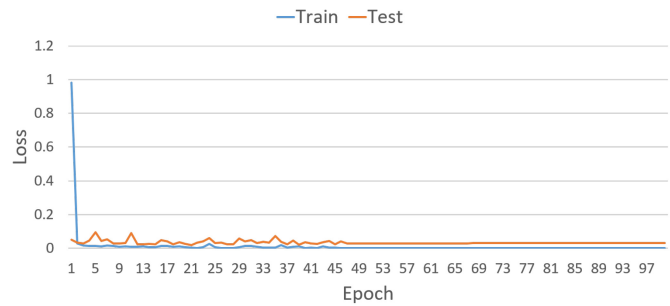


Fig. 13. Loss variation with respect to train and test data sets.

The state-of-the-art SL estimation method proposed by Hannink *et al.* [25] is implemented with our data set as the benchmark. For another comparative experiment, we use the same multimodality architecture but treat the left and right inputs as the same inputs instead of using multitasks learning concepts. We named this experiment “Proposed Combined.” Fig. 12 and Table VI present the evaluation of the regression models in terms of the proposed evaluation metrics.

As we can see, the proposed and the proposed combined methods outperform the benchmark because the introduction of pressure sensors brings more feature information that can contribute to model optimization. Furthermore, the proposed method has better outcomes than the proposed combined method. Since the sensors’ placements on the left and right foot are symmetrical, there could be a different regression task when using the features, even though they share similar features.

| | Down Ramp | Down Stairs | Walking | Jogging | Sit-to-Stand | Slippery Floor | Up Ramp | Up Stairs | Side Stepping | Obstacle | Precision |
|----------------|-----------|-------------|---------|---------|--------------|----------------|---------|-----------|---------------|----------|-----------|
| Down Ramp | 68 | 0 | 0 | 0 | 0 | 0 | 0 | 0 | 0 | 0 | 0.82 |
| Down Stairs | 0 | 51 | 0 | 0 | 0 | 0 | 0 | 0 | 0 | 2 | 1 |
| Walking | 13 | 0 | 895 | 0 | 0 | 1 | 28 | 0 | 0 | 1 | 0.99 |
| Jogging | 0 | 0 | 0 | 284 | 0 | 0 | 0 | 0 | 0 | 1 | 1 |
| Sit-to-Stand | 0 | 0 | 0 | 0 | 960 | 3 | 0 | 1 | 1 | 0 | 0.98 |
| Slippery Floor | 0 | 0 | 0 | 0 | 3 | 1834 | 0 | 1 | 3 | 38 | 0.97 |
| Up Ramp | 0 | 0 | 0 | 0 | 0 | 0 | 45 | 0 | 0 | 0 | 0.44 |
| Up Stairs | 0 | 0 | 0 | 0 | 0 | 0 | 1 | 52 | 0 | 0 | 0.85 |
| Side Stepping | 0 | 0 | 0 | 0 | 0 | 4 | 0 | 0 | 827 | 1 | 0.99 |
| Obstacle | 2 | 0 | 11 | 0 | 14 | 41 | 28 | 7 | 2 | 1872 | 0.98 |
| Recall | 1 | 0.96 | 0.95 | 1 | 0.99 | 0.98 | 1 | 0.98 | 0.99 | 0.95 | |

Fig. 14. Confusion matrix related to the whole test set.

TABLE VII
COMPOSITION OF THE GAIT REEDUCATION ACTIVITY DATA SET

| Activity | ID | Number of Instances |
|---------------------------|----|---------------------|
| Down-ramp | 1 | 470 |
| Downstairs | 2 | 455 |
| Walking | 3 | 1340 |
| Jogging | 4 | 687 |
| Sit-to-stand | 5 | 1367 |
| Walking on slippery floor | 6 | 2281 |
| Up-ramp | 7 | 447 |
| Upstairs | 8 | 455 |
| Sidestep Walking | 9 | 1234 |
| Overcome obstacles | 10 | 2379 |

C. Gait Reeduction Activity Classification

To evaluate the performance of the proposed multimodality classification model, three different experiments are implemented.

In the first scenario, we classify all processed data into categories according to the activity types. Table VII lists the number of instances included in each activity type. To avoid the overfitting issue caused by data imbalance, we ensure all the classes have equal instances for training. Therefore, the sample size of the class that has fewer instances is selected as the benchmark. 90% of the benchmark value is designated as the number of instances that should be selected from each class. Then, the rest instances are used for test. Finally, there are 4020 instances for train and 7095 instances for test.

Fig. 14 illustrates the variation in loss function concerning train and test set. As the figure presents, the loss for train data decreases very fast within the first five iterations, and reaches a stable regime after 45 iterations. The loss for the test set fluctuates within the first 45 iterations. It decreases to a small value with the training loss gradually reaches its stable regime.

TABLE VIII
ACCURACY OF LEAVE-ONE-OUT TESTING

| Test ID | Accuracy (%) |
|----------|--------------|
| 1 | 98.47 |
| 2 | 95.47 |
| 3 | 96.78 |
| 4 | 98.18 |
| 5 | 97.22 |
| Averaged | 97.22 |

TABLE IX
COMPARISONS OF DIFFERENT TYPES OF SENSOR DATA INPUT FOR THE MODEL

| Input Sensor Data Types | Accuracy (%) |
|-------------------------|--------------|
| Pressure, Acc, Gyro | 97.08 |
| Pressure | 91.95 |
| Acc, Gyro | 92.38 |

Fig. 12 presents the evaluation of the classification model from the aspect of the confusion matrix, precision, and recall.

In the second scenario, we investigate the model's robustness via data variance from subject to subject. We randomly select one subject's data as a test set, and the rest subjects' data are used for training. We run the method five times. Values of accuracy from the five experiments are summarized to evaluate the model's robustness, shown in Table VIII. The accuracy is pretty high from subject to subject test, demonstrating that our model is robust in facing sample divergence.

In the third scenario, we take the sensor-measurements separately as the models' input sequences. One uses the under-feet pressure sensors as the model's input sequences, and the other is using both Acc and Gyro as the model's input sequences. The purpose of the comparative experiments is to demonstrate that multimodality deep convolutional neural network is a promising model for gait-related activities classification.

Table IX summarizes the performances of the models with different types of sensor-measurements input. From Table IX, we can see that our proposed method outperforms the other ones greatly.

V. CONCLUSION

In this article, we proposed the multimodality deep learning approach based on our wearable gait lab system to investigate SL estimation and rehabilitation activity recognition applications. The entire system integrated mobile sensing, information logging, mobile data visualization, and learning analysis. Two data sets gathered by this system are used to validate the works. The proposed methods have been proven to estimate complicated changing SLs and classify ten gait rehabilitation activities with very high accuracy. Consequently, the entire system is more applicable for clinically relevant gait monitoring and gait analysis.

ACKNOWLEDGMENT

The funders had no role in the study design; data collection, analysis, or interpretation; in the writing of the report; or in the decision to submit the article for publication.

REFERENCES

- [1] P. Mahlknecht *et al.*, "Prevalence and burden of gait disorders in elderly men and women aged 60–97 years: A population-based study," *PLoS One*, vol. 8, no. 7, 2013, Art. no. e69627.
- [2] C. Miller-Patterson, R. Buesa, N. McLaughlin, R. Jones, U. Akbar, and J. H. Friedman, "Motor asymmetry over time in Parkinson's disease," *J. Neurol. Sci.*, vol. 393, pp. 14–17, Oct. 2018.
- [3] T. A. Boonstra, H. van der Kooij, M. Munneke, and B. R. Bloem, "Gait disorders and balance disturbances in Parkinson's disease: Clinical update and pathophysiology," *Current Opinion Neurol.*, vol. 21, no. 4, pp. 461–471, 2008.
- [4] T. Ellis, J. T. Cavanaugh, G. M. Earhart, M. P. Ford, K. B. Foreman, and L. E. Dibble, "Which measures of physical function and motor impairment best predict quality of life in parkinson's disease?" *Parkinsonism Related Disord.*, vol. 17, no. 9, pp. 693–697, 2011.
- [5] "Elliptical Machines: Why Stride Length Is Important." [Online]. Available: <https://www.toptenreviews.com/health/articles/elliptical-machines-why-stride-length-is-important/> (accessed Jan. 10, 2021).
- [6] "How to Calculate Stride Length and Step Length." [Online]. Available: <https://www.healthline.com/health/stride-length> (accessed Jan. 13, 2021).
- [7] E. Rastegari, V. Marmelat, L. Najjar, D. Bastola, and H. H. Ali, "Using gait parameters to recognize various stages of Parkinson's disease," in *Proc. IEEE Int. Conf. Bioinform. Biomed. (BIBM)*, 2017, pp. 1647–1651.
- [8] L. Hak, H. Houdijk, P. J. Beek, and J. H. van Dieën, "Steps to take to enhance gait stability: The effect of stride frequency, stride length, and walking speed on local dynamic stability and margins of stability," *PLoS One*, vol. 8, no. 12, 2013, Art. no. e82842.
- [9] A.-M. Ferrandez and O. Blin, "A comparison between the effect of intentional modulations and the action of l-dopa on gait in parkinson's disease," *Behav. Brain Res.*, vol. 45, no. 2, pp. 177–183, 1991.
- [10] D. Chen, Y. Cai, and M.-C. Huang, "Customizable pressure sensor array: Design and evaluation," *IEEE Sensors J.*, vol. 18, no. 15, pp. 6337–6344, Aug. 2018.
- [11] D. Chen *et al.*, "Bring gait lab to everyday life: Gait analysis in terms of activities of daily living," *IEEE Internet Things J.*, vol. 7, no. 2, pp. 1298–1312, Feb. 2020.
- [12] R. E. Rifkin *et al.*, "Use of a pressure-sensing walkway system for biometric assessment of gait characteristics in goats," *PLoS ONE*, vol. 14, no. 10, 2019, Art. no. e0223771.
- [13] M. Oosterlinck, F. Pille, D. C. Sonneveld, A. M. Oomen, F. Gasthuys, and W. Back, "Contribution of dynamic calibration to the measurement accuracy of a pressure plate system throughout the stance phase in sound horses," *Vet. J.*, vol. 193, no. 2, pp. 471–474, 2012.
- [14] W. Wang, A. X. Liu, and M. Shahzad, "Gait recognition using wifi signals," in *Proc. ACM Int. Joint Conf. Pervasive Ubiquitous Comput.*, 2016, pp. 363–373.
- [15] A.-K. Seifert, A. M. Zoubir, and M. G. Amin, "Detection of gait asymmetry using indoor doppler radar," in *Proc. IEEE Radar Conf. (RadarConf)*, 2019, pp. 1–6.
- [16] S. Zhang, Y. Xiong, J. Ma, Z. Song, and W. Wang, "Indoor location based on independent sensors and WiFi," in *Proc. Int. Conf. Comput. Sci. Netw. Technol.*, vol. 4, 2011, pp. 2640–2643.
- [17] J. Zhang *et al.*, "Gate-ID: Wifi-based human identification irrespective of walking directions in smart home," *IEEE Internet Things J.*, vol. 8, no. 9, pp. 7610–7624, May 2021.
- [18] C. Wu, F. Zhang, Y. Hu, and K. J. R. Liu, "GaitWay: Monitoring and recognizing gait speed through the walls," *IEEE Trans. Mobile Comput.*, vol. 20, no. 6, pp. 2186–2199, Jun. 2021.
- [19] A. Rampp, J. Barth, S. Schlein, K. Gamann, J. Klucken, and B. M. Eskofier, "Inertial sensor-based stride parameter calculation from gait sequences in geriatric patients," *IEEE Trans. Biomed. Eng.*, vol. 62, no. 4, pp. 1089–1097, Apr. 2015.
- [20] Q. Wang, L. Ye, H. Luo, A. Men, F. Zhao, and Y. Huang, "Pedestrian stride-length estimation based on LSTM and denoising autoencoders," *Sensors*, vol. 19, no. 4, p. 840, 2019.
- [21] A. Muro-De-La-Herran, B. Garcia-Zapirain, and A. Mendez-Zorrilla, "Gait analysis methods: An overview of wearable and non-wearable systems, highlighting clinical applications," *Sensors*, vol. 14, no. 2, pp. 3362–3394, 2014.
- [22] F. Horak, L. King, and M. Mancini, "Role of body-worn movement monitor technology for balance and gait rehabilitation," *Phys. Ther.*, vol. 95, no. 3, pp. 461–470, 2015.
- [23] I. Mileti, J. Taborri, S. Rossi, M. Petrarca, F. Patanè, and P. Cappa, "Evaluation of the effects on stride-to-stride variability and gait asymmetry in children with cerebral palsy wearing the wake-up ankle module," in *Proc. IEEE Int. Symp. Med. Meas. Appl. (MeMeA)*, 2016, pp. 1–6.
- [24] J. Shah *et al.*, "Increased foot strike variability in Parkinson's disease patients with freezing of gait," *Parkinsonism Related Disord.*, vol. 53, pp. 58–63, Aug. 2018.
- [25] J. Hannink *et al.*, "Mobile stride length estimation with deep convolutional neural networks," *IEEE J. Biomed. Health Inform.*, vol. 22, no. 2, pp. 354–362, Mar. 2018.
- [26] H. Jiang, Y. Cai, X. Zeng, and M.-C. Huang, "Does background really matter? worker activity recognition in unconstrained construction environment," in *Proc. IEEE 15th Int. Conf. Wearable Implantable Body Sensor Netw. (BSN)*, 2018, pp. 50–53.
- [27] A. Avci, S. Bosch, M. Marin-Perianu, R. Marin-Perianu, and P. Havinga, "Activity recognition using inertial sensing for healthcare, wellbeing and sports applications: A survey," in *Proc. 23th Int. Conf. Architect. Comput. Syst.*, 2010, pp. 1–10.
- [28] C. Zhang and Y. Tian, "RGB-D camera-based daily living activity recognition," *J. Comput. Vis. Image Process.*, vol. 2, no. 4, p. 12, 2012.
- [29] W. Niu, J. Long, D. Han, and Y.-F. Wang, "Human activity detection and recognition for video surveillance," in *Proc. IEEE Int. Conf. Multimedia Expo (ICME)*, vol. 1, 2004, pp. 719–722.
- [30] D. L. Jaffe, D. A. Brown, C. D. Pierson-Carey, E. L. Buckley, and H. L. Lew, "Stepping over obstacles to improve walking in individuals with poststroke hemiplegia," *J. Rehabil. Res. Develop.*, vol. 41, pp. 283–292, May 2004.
- [31] J. P. Gupta, N. Singh, P. Dixit, V. B. Semwal, and S. R. Dubey, "Human activity recognition using gait pattern," *Int. J. Comput. Vis. Image Process.*, vol. 3, no. 3, pp. 31–53, 2013.
- [32] I. H. Lopez-Nava, M. Garcia-Constantino, and J. Favela, "Recognition of gait activities using acceleration data from a smartphone and a wearable device," *Multidiscipl. Digit. Publ. Inst. Proc.*, vol. 31, no. 1, p. 60, 2019.
- [33] R. Riener, M. Rabuffetti, and C. Frigo, "Stair ascent and descent at different inclinations," *Gait Posture*, vol. 15, no. 1, pp. 32–44, 2002.
- [34] T. F. Novacheck, "The biomechanics of running," *Gait Posture*, vol. 7, no. 1, pp. 77–95, 1998.
- [35] W.-R. Chang, C.-C. Chang, M. F. Lesch, and S. Matz, "Gait adaptation on surfaces with different degrees of slipperiness," *Appl. Ergonom.*, vol. 59, pp. 333–341, Mar. 2017.
- [36] M. W. Whitmore, L. J. Hargrove, and E. J. Perreault, "Gait characteristics when walking on different slippery walkways," *IEEE Trans. Biomed. Eng.*, vol. 63, no. 1, pp. 228–239, Jan. 2016.

- [37] "Gait-Side Stepping." [Online]. Available: https://careguides-videos.med.umich.edu/media/Gait+-+Side+Stepping/1_lqt4vdyu/44536641 (accessed Jan. 15, 2021).
- [38] "Pytorch." [Online]. Available: <https://pytorch.org/> (accessed Jan. 15, 2021).
- [39] J. Barth *et al.*, "Stride segmentation during free walk movements using multi-dimensional subsequence dynamic time warping on inertial sensor data," *Sensors*, vol. 15, no. 3, pp. 6419–6440, 2015.



Yi Cai received the Ph.D. degree in electrical engineering from the Electrical Engineering and Computer Science Department, Case Western Reserve University, Cleveland, OH, USA, in 2021.

He has been involved in the NSF sponsored Project, focusing on the experiment simulation and hardware and software system design. His research interests are in the field of mobile health, machine learning, sensor data analysis, and wearable sensor network.



Xiaoye Qian received the M.S. degree from the Electrical Engineering and Computer Science Department, Case Western Reserve University, Cleveland, OH, USA, in 2019, where he is currently pursuing the Ph.D. degree in computer engineering.

His major research areas are mobile health, computer vision, and big data analysis.



Huiyi Cao received the M.S. degree in computer science from the Computer and Data Sciences Department, Case Western Reserve University, Cleveland, OH, USA, in 2020.

Her current research interests include mobile health software development and data analysis.



Jianian Zheng received the M.S. degree in computer science from the Computer and Data Sciences Department, Case Western Reserve University, Cleveland, OH, USA, in 2020.

His research interests include machine learning, data mining, and data visualization in healthcare.



Wenyao Xu received the bachelor's and master's degrees from Zhejiang University, Hangzhou, China, in 2006 and 2008, respectively, and the Ph.D. degree from the University of California at Los Angeles, Los Angeles, CA, USA, in 2013.

He is an Associate Professor (Tenure) with the Computer Science and Engineering Department, University at Buffalo (SUNY), Buffalo, NY, USA. His research has focused on exploring novel sensing and computing technologies to build up innovative Internet of Things systems for high-impact human-technology applications in the fields of smart health and cybersecurity. Results have been published in peer-reviewed top research venues across multiple disciplines. To date, his group has published over peer-reviewed 200 papers, won 14 best paper awards, three best paper nominations, and three international best design awards. His inventions have been filed within U.S. and internationally as patents, and have been licensed to industrial players. His research has been reported in high-impact media outlets.

Dr. Xu has served as an Associate Editor in multiple journals, including *IEEE TRANSACTIONS ON BIOMEDICAL CIRCUITS AND SYSTEMS* and *IEEE Internet of Things Journal*. He also serves the organizing role of numerous conferences in the field of Smart Health and Internet of Things, including the TPC Chair for IEEE/ACM CHASE'22 and IEEE BSN'2018.



Ming-Chun Huang received the B.S. degree in electrical engineering from Tsing Hua University, Hsinchu, Taiwan, in 2007, the M.S. degree in electrical engineering from the University of Southern California, Los Angeles, CA, USA, in 2010, and the Ph.D. degree in computer science from the University of California at Los Angeles, Los Angeles, in 2014.

Prior to joining Duke Kunshan University, Suzhou, China, he was an Associate Professor with Case Western Reserve University, Cleveland, OH, USA, and the Director of the Mobile Health Laboratory and the Sensing and Interaction Laboratory from 2014 to 2021. He had over 14 years of research experience conducting interdisciplinary scientific projects with researchers from distinct areas (e.g., Biomedical Engineering, Medicine, and Nursing). He had successfully administered past funded projects (e.g., manufacturing costs, staffing, research protections, and budget) and productively published over 80 peer-reviewed publications. His inventions have been filed internationally as patents and have been licensed to industrial players. His research has been reported in over hundreds of high-impact media outlets. For the nature of richness and high impact of the research topics he was involved in, his research results in a plethora of new knowledge in aspects ranging from innovative IoT sensing technology, closed-loop AI analytics methodology, optimized clinical decision making, and just-in-time users' risk assessment. His research focus is the intersection among Internet of Things, smart health, machine learning and informatics, motion, and physiological signal sensing.